Letter

Braiding topology of non-Hermitian open-boundary bands

Yongxu Fu [*] and Yi Zhang [†]
International Center for Quantum Materials, School of Physics, Peking University, Beijing 100871, China

(Received 27 May 2024; revised 12 August 2024; accepted 13 August 2024; published 5 September 2024)

There has been much recent interest and progress on topological structures of the non-Hermitian Bloch bands. Here, we study the topological structures of non-Bloch bands of non-Hermitian multiband quantum systems under open boundary conditions, which has received limited attention in prior studies. Using a continuity criterion and an efficient sub-generalized Brillouin zone (sub-GBZ) algorithm, we establish a homotopic characterization—braiding topology, e.g., characterized by the band's total vorticity—for open-boundary bands and sub-GBZs. Such topological identification is robust without topological transition and emergent degenerate points, such as exceptional points. We further analyze the transition's impact on bands and spectral flows, including interesting properties unique to open boundaries, and numerically demonstrate our conclusions with tight-binding model examples. We unveil a crucial insight that open-boundary bands interchange their portions after encountering certain exceptional points. Our results enrich the foundational understanding of topological characterizations for generic non-Hermitian quantum systems.

DOI: 10.1103/PhysRevB.110.L121401

Introduction. The Bloch band theory is a well-established cornerstone in solid-state physics [1–7]. In the past few years, research on non-Hermitian quantum systems has made the extension of such band theory a major focus [8–18]. For instance, a non-Bloch band theory has been developed for one-dimensional (1D) non-Hermitian quantum systems under open boundary condition (OBC) [19–28] and rapidly verified in various experimental platforms [29–37]. Superseding the conventional Brillouin zone (BZ), the non-Bloch band theory's generalized Brillouin zone (GBZ) gives rise to the non-Hermitian skin effect and breaks down the bulk-boundary correspondence [38–41]. Further generalizations have also been made to higher dimensions [42–53] and scale-free localization scenarios [54–59].

Topological concepts such as the braid groups and the knots [60,61] have had widespread and fruitful applications in various physics topics. The nodal-line knots of topological semimetals [62–65] are soon followed by the exceptional-line knots in non-Hermitian systems [66–79]. Braid and knot structures also emerge in the three-dimensional (3D) space spanned by the complex energy and the wave vector of the Bloch band theory [80–91], applicable only for periodic boundary conditions (PBC). However, despite recent work on similar topology for non-Bloch bands under OBC [92], the general definition and properties remain unclear, especially for generic non-Hermitian systems with multiple non-Bloch bands with respective GBZs dubbed the sub-GBZs [24–26].

In this paper, we propose a continuity criterion and a homotopic formalism of the braid and knot topology for the non-Bloch bands of non-Hermitian quantum systems under OBC in the thermodynamic limit, even in the presence of multiple bands and sub-GBZs. Consequently, we can characterize such robust topology and the intermediate topological transitions, denoted by the emergence of exceptional points (EPs), by the non-Bloch bands' vorticity. We have also established an efficient and accurate numerical algorithm, demonstrated examples of non-Hermitian multiband models, and pointed out their intriguing characteristics unique to OBCs. We reveal that open-boundary bands interchange their parts as the system crosses particular EPs. Additionally, compared to PBC bands, the braiding of non-Hermitian OBC bands is significant due to its more diverse transition options—the commonly two-visit OBC eigenvalues offer multiple choices for exchange partners and flow directions at the transition. Our results offer an essential facet and thus pave the way toward our full understanding of the topology of generic non-Hermitian quantum systems under OBC.

Continuity criterion of bulk energy bands under OBC. Consider a generic 1D noninteracting non-Hermitian tight-binding Hamiltonian:

$$\hat{\mathcal{H}} = \sum_j \sum_{m=-\mathcal{R}_1}^{\mathcal{R}_2} \mathbf{c}_j^\dagger \mathcal{T}_m \mathbf{c}_{j+m}, \tag{1}$$

with N lattice sites (unit cells) and n internal degrees of freedom on each site j—the dimension of the hopping matrices $\mathcal{T}_m$. Without loss of generality, we set the hopping ranges $\mathcal{R}_1 = \mathcal{R}_2 \equiv \mathcal{R}$. The direct diagonalization of such a non-Hermitian $\hat{\mathcal{H}}$ suffers from precision issues, especially for large system sizes [93]. Instead, the energy bands of $\hat{\mathcal{H}}$ may descend from the roots of the characteristic equation with respect to the reference energy E:

$$f(\beta, E) \equiv \det[\mathcal{H}(\beta) - E \times \mathbb{1}_{n\times n}] = 0, \tag{2}$$

[*]Contact author: yongxufu@pku.edu.cn
[†]Contact author: frankzhangyi@gmail.com

where $\mathcal{H}(\beta)=\sum_{m=-\mathcal{R}}^{\mathcal{R}}\mathcal{T}_m\beta^m$ is a matrix-valued Laurent polynomial of the complex variable β. In the presence of translation symmetry and PBC, the Bloch band theory dictates $\beta=e^{ik}$, where the wave vector (lattice momentum) $k\in[-\pi,\pi]$ is defined within the (first) BZ [94]. For OBC, on the other hand, we need to adapt to the non-Bloch band theory [20,21], where β's satisfy the GBZ condition—the $2M\equiv 2n\mathcal{R}$ sorted roots of the characteristic Eq. (2), $|\beta_1|\leqslant|\beta_2|\leqslant\cdots\leqslant|\beta_{2M}|$, obey $|\beta_M|=|\beta_{M+1}|$. The bulk energy bands follow such BZs or GBZs accordingly. Throughout this paper, we refer to k as the wave vector in the BZ of the Bloch band theory under PBC, while θ represents the complex argument of β in the GBZ of the non-Bloch band theory under OBC.

Noteworthily, each OBC band ε_i, $i=1,2,\dots,n$, is related to an ideally unique continuous sub-GBZ $\mathcal{C}_i$ for a generic non-Hermitian system in the thermodynamic limit [24–26], disregarding the potential emergence of pseudogaps with a very low density of states [95]. However, due to the multiplicity of the roots of the characteristic Eq. (2), subtle complications may arise when we associate the OBC bands with the sub-GBZs. For instance, while the auxiliary GBZ (aGBZ) can give all of the sub-GBZs [24], isolating the multivalued energy bands for each sub-GBZ remains uncontrolled in practice and thus intractable for generic non-Hermitian Hamiltonians except for certain simple cases [26]. Here, we overcome such ambiguity by enforcing the continuity criterion that a map from the sub-GBZ $\mathcal{C}_i$ to the OBC band ε_i must be continuous. In other words, we require that infinitesimal variations on $\mathcal{C}_i$ only induce infinitesimal variations in ε_i [96], which keep the bands' clear distinctions despite coincidental roots thus intersecting sub-GBZs.

Here, we propose an algorithm to enforce such a continuity criterion. First, we solve the resultant equation,

$$\mathcal{R}_E[f(\beta,E),f(\beta e^{i\Theta},E)]=0, \tag{3}$$

over the range $\Theta\in[-\pi,\pi]$. Here, $\mathcal{R}_E$ represents the resultant of $f(\beta,E)$ and $f(\beta e^{i\Theta},E)$ relative to E [97,98]. For a given Θ, the characteristic equations $f(\beta,E)=0$ and $f(\beta e^{i\Theta},E)=0$ share a common energy E if and only if the resultant Eq. (3) holds. Thus, we can obtain all $\beta_{p+1}=\beta_p e^{\pm i\Theta}$ solutions satisfying the characteristic Eq. (2), so that $|\beta_1|\leqslant\cdots\leqslant|\beta_p|=|\beta_{p+1}|\leqslant\cdots\leqslant|\beta_{2M}|$, $p=1,2,\dots,2M-1$, for a specific Θ. Next, we select the β solutions with $p=M$, which coincide with the GBZ condition, and map out the GBZ as we vary Θ. Finally, after obtaining the set of GBZ with the corresponding ensemble of OBC bands, we apply the continuity criterion: as the argument θ of β increases, both β_i and ε_i within each band i evolve continuously. In practice, it helps to separate this ensemble of energies into individual bands ε_i one by one, following the order of β's argument at a specific numerical precision. Each $\{\beta_i\}$ for $\theta\in[-\pi,\pi]$ constitutes a sub-GBZ $\mathcal{C}_i$. Such an algorithm can effectively and unambiguously determine the multiple OBC bands and the associated sub-GBZs, except for the degenerate points (DPs) where multiple β_i coincide and signal a topological transition; see detailed elucidation of the algorithm along with the examples and applications later and in the Supplemental Material [93].

We note that although the mapping from $\mathcal{C}_i$ to ε_i is continuous (and vice versa), it is not homeomorphic or injective but rather surjective. Namely, an E value may correspond to two (or more) points on $\mathcal{C}_i$, dubbed as a two-bifurcation (or $\mathfrak{n}$-bifurcation) point [26,27], and passed through two (or $\mathfrak{n}$) times as we move across $\mathcal{C}_i$. We note that the $\mathfrak{n}$-bifurcation point is usually within a single band and not a degeneracy between the bands. The degeneracy between two or more bands will grant interesting physical consequences, such as topological transitions and DPs, as we discuss next.

Band braiding topology with sub-GBZs. The continuity criterion yields continuous OBC bands $\varepsilon_i(\beta)$ with β lying on the related sub-GBZ $\mathcal{C}_i$. For simplicity, we only consider cases where all sub-GBZs are closed, i.e., homeomorphic to the one-sphere S^1, and $r=|\beta|$ is a single-valued function of θ on each $\mathcal{C}_i$ in the main text. We also choose the same convention of θ, i.e., identical starting points θ_0, for all sub-GBZs' arguments so that β remains consistent and continuous before and after a topological transition, where parts of the OBC bands may switch their partners. We discuss more complex cases with intertwined sub-GBZs in the Supplemental Material [93].

The braiding topology is only available to multiband systems. We define two arbitrary bands $i\neq j$ as isolated if $\varepsilon_i(\beta_1)\neq\varepsilon_j(\beta_2)$ for any $\beta_{1,2}\in\mathcal{C}_{i,j}$, separated if they are not isolated yet $\varepsilon_i(\beta)\neq\varepsilon_j(\beta)$ for any coincidental $\beta\in\mathcal{C}_{i,j}$, and degenerate if $\varepsilon_i=\varepsilon_j$ at at least one degenerate point (DP) $\beta_i=\beta_j$ on $\mathcal{C}_{i,j}$. We wish to analyze the equivalence classes of the OBC bands $\varepsilon_i(\beta)$ in the absence of multiband degeneracies. However, as long as $\varepsilon_i=\varepsilon_j$ and $\theta_i=\theta_j$, we obtain $|\beta_i|=|\beta_j|$ as dictated by the GBZ condition, and then $\beta_i=\beta_j$; therefore, it suffices to relate the transition to $\varepsilon_i(\theta)$ instead of $\varepsilon_i(\beta)$ and focus instead on the continuous mapping from $\theta\in S^1$ to the OBC energies $\varepsilon_i\in\mathbb{C}$. The subsequent homotopy characterization resembles that of a non-Hermitian Bloch Hamiltonian $\mathcal{H}(k)$ with the lattice momentum $k\in[-\pi,\pi]$ within the BZ [80–82,88] in our place of θ.

Strictly speaking, the relevant nonbased map is from S^1 to $\mathcal{X}_n=(\mathrm{Conf}_n\times F_n)/\mathcal{S}_n$, where $(\varepsilon_1,\dots,\varepsilon_n)\in\mathrm{Conf}_n$ is the ordered n tuples of the complex energies, the quotient space $F_n=\mathrm{GL}_n(\mathbb{C})/\mathrm{GL}_1^n(\mathbb{C})$ describes the eigenvectors of $\mathcal{H}(\beta_i)$ with respect to the complex energies, and $\mathcal{S}_n$ is the permutation group. The homotopy equivalence classes $[S^1,\mathcal{X}_n]$ can be simplified as the conjugacy classes of the braid group $B_n=\pi_1(\mathrm{Conf}_n/\mathcal{S}_n)$ due to $\pi_1(F_n)=0$, and further reduced to the pure braid group PB_n, a subgroup of B_n, for the closed sub-GBZs and S^1 manifold here. Notably, it is unnecessary to specify the starting point of S^1 in the homotopy characterization, as different choices correspond to braids within the same conjugacy class. More complicated scenarios with intertwined sub-GBZs and B_n braid group classifications are in the Supplemental Material [93].

Intuitively, the target B_n conjugacy classes are equivalent to the geometric knots [99] of strings ($i=1,2,\dots,n$) in the $(\mathrm{Re}(\varepsilon),\mathrm{Im}(\varepsilon),\theta)$ 3D space, and the target PB_n to the geometric knots of closed loops [60,61,82] in the 3D space periodic in $\theta\in[-\pi,\pi]$. We may thus characterize the braiding topology of the OBC bands with the total vorticity over the bands,

$$\nu=\frac{1}{2}\sum_{i\neq j}\nu_{ij}, \tag{4}$$

relevant to the braid crossings [93], where ν_{ij} is the vorticity between two bands $\varepsilon_i(\theta)$ and $\varepsilon_j(\theta)$ [100],

$$\nu_{ij} = \frac{1}{2\pi}\oint_{S^1}\frac{d}{d\theta}\arg[\varepsilon_i(\theta)-\varepsilon_j(\theta)]d\theta, \tag{5}$$

in a similar way to the non-Hermitian Bloch bands. We note that the vorticity is not a complete characterization of the braiding topology, and a comprehensive description requires braid words [60,61,82] or knot invariants (polynomials), e.g., the Jones polynomials [70,101–103], to encode the full information of the braiding topology. Topologically different braids may manifest the same vorticity [76]; nevertheless, braids with distinct vortices must be topologically different, which offers us an elementary way to distinguish the different braiding topology. For more complex scenarios, knot polynomials might be necessary, but the overall braiding topology and phase transition presented in this paper remain valid.

Topological transition of OBC band braiding. The DPs are commonly EPs, which are stable, or unstable degenerate points (UDPs), which rely on fine-tuning and are unstable and evolve into several EPs upon generic perturbations [82,93,104–107]. Isolated bands are always topologically trivial, while separated bands may host nontrivial braiding topology, e.g., finite vorticity, which remains robust and protected without going through DPs. Correspondingly, the degenerate bands denote the critical point of a topological transition, where the vorticity may undergo a change.

For instance, we illustrate the different OBC band braidings and the topological transition in between on a two-parameter ($\gamma_{1,2}$) phase diagram in Fig. 1(a), where a twofold degeneracy occurs on the critical line. We note that a higher-fold degeneracy can split into several robust twofold degeneracies upon perturbations. Without loss of generality, we consider two types of transition: the degeneracy is introduced by stable EPs [along the l_e line in Fig. 1(a)] or UDPs [along the l_u line in Fig. 1(a)]. Without extra symmetries [104–107], a UDP splits into two EPs upon a small perturbation, e.g., finite γ_2.

Upon crossing each EP, two bands interchange and introduce a vorticity change of $\Delta\nu_e = \pm 1/2$. To see that, consider the effective Hamiltonian upon the two relevant bands close to the stable EP: $\mathcal{H}_{\rm eff} = h_x\sigma_x + h_y\sigma_y + h_z\sigma_z$, where $\sigma_{x,y,z}$ are the Pauli matrices and $h_{x,y,z}$ are small parameters depending on θ and $\gamma_{1,2}$. The two bands $E_\pm = \pm(h_x^2+h_y^2+h_z^2)^{1/2}$ follow a multivalued function with a branch cut originating from the EP at $h_x^2+h_y^2+h_z^2=0$; see an example Riemann surface structure in the vicinity of the EP as a function of θ and a model parameter, e.g., γ_2, in Fig. 1(c). Any closed contour around the EP will traverse the branch cut and switch one band with the other, introducing a vorticity change of $\Delta\nu_e = \pm 1/2$ and indicating such an EP's stability against perturbations unless annihilated or merged with another EP [93].

After the topological transition, the two bands separate once again, but there may be a resulting change of total vorticity and an exchange of partners between parts of the bands. As we sum up θ for the total vorticity, the difference between the neighboring models [brown contours in Figs. 1(a1) and 1(a2)] receives contributions from all intermediate DPs (magenta circles): $\nu_2 - \nu_1 = \sum\Delta\nu$. For instance, two EPs with $\Delta\nu = -1/2$ allow a difference of -1 between the total

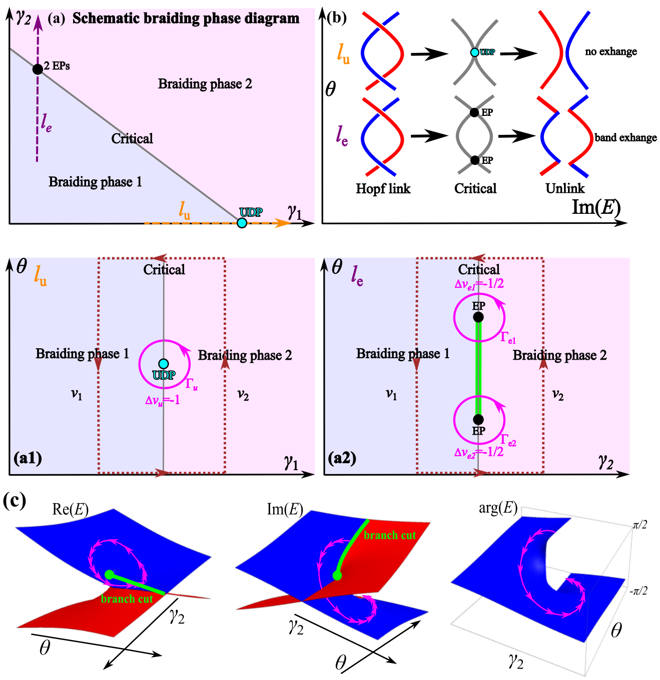

FIG. 1. (a) A schematic phase diagram shows non-Hermitian models with different OBC band braidings are separated by intermediate topological transitions via UDP (orange arrowed line l_u) or EPs (purple arrowed line l_e). (b) The topological transition of OBC bands $\varepsilon_{1,2}$ from a Hopf link to an unlink may either go through a UDP directly or a pair of EPs, which exchange the bands between the EPs. The resulting change in total vorticity from ν_1 to ν_2 (brown dashed lines) corresponds to the contours around all DPs, (a1) a UDP with $\Delta\nu_u = -1$ or (a2) two EPs with $\Delta\nu_e = -1/2$ each and a branch cut in between (thick green line). (c) The Riemann surface structure shows the exchange between the two bands (blue and red surfaces) and the vorticity change as the contour (magenta arrowed curve) circles a single EP.

vorticity of the models on two sides, e.g., a Hopf link and an unlink in Fig. 1(b), upon tuning the model parameter γ_2. In addition, after the two bands $\varepsilon_{1,2}$ touch at the two EPs, they separate and enter the unlink region, yet with their parts between the two EPs interchanged; see the lower panel in Fig. 1(b).

On the other hand, topological transitions through EPs are not the only option, as a change of total vorticity can also happen via UDPs with $|\Delta\nu_u| \geqslant 1$, which may separate into multiple EPs. For example, the UDP with vorticity $\Delta\nu_u = -1$ [Fig. 1(a1)] can split into two separate EPs with $\Delta\nu_e = -1/2$ each and a branch cut in between [Fig. 1(a2)] upon perturbations. Similarly, we can visualize such a UDP as two $\Delta\nu_e = -1/2$ EPs merged together, leaving behind no branch cut or band exchange. Correspondingly, during the transition from the Hopf link to the unlink through a UDP [upper panel in Fig. 1(b)], the two bands ε_1 and ε_2 merely touch at the UDP and directly move across without any band exchanges, yielding an unlink afterward. The stable twofold degeneracies constitute the fundamental ingredient of the braiding transition. Therefore, the braiding transition in non-Hermitian models with more than two bands

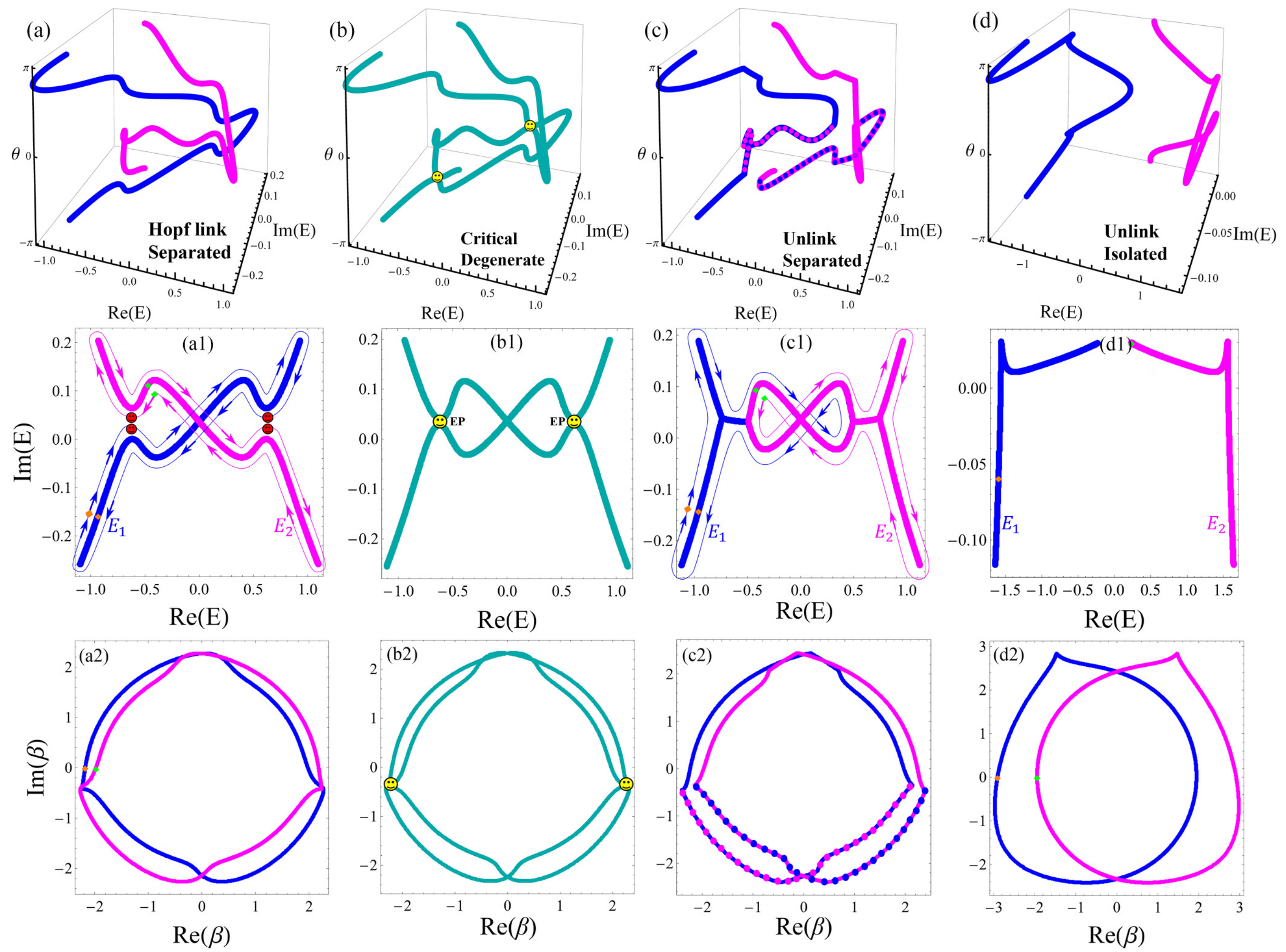

FIG. 2. The OBC bands of the non-Hermitian model in Eq. (6) demonstrate clear braiding topology in the $(\mathrm{Re}(E), \mathrm{Im}(E), \theta)$ space: (a) a Hopf link at $\lambda_3 = 0.36$; (b) a topological transition with two emergent EPs (yellow points) at $\lambda_3 \approx 0.375$; (c) a separated unlink at $\lambda_3 = 0.4$; and (d) an isolated unlink at $\lambda_3 = 1$. $\lambda_1 = \lambda_2 = 0$, $t_p = 0.15$, $t_m = 0.85$, $t_a = 0.2$, and $m = 0.1$. We also show (a1)–(d1) the corresponding bands $E_{1,2}$ in the complex E plane and (a2)–(d2) the sub-GBZs $\mathcal{C}_{1,2}$ in the complex β plane. The blue and magenta arrows show the spectral flows as θ evolves along the sub-GBZs, where the orange and green diamonds mark the $\theta = -\pi$ locations. Note that the "∞"-shaped central loop in (c1) is visited once only by each band, which overlaps there. The magenta (blue) dots in (c) and (c2) denotes the parts of the bands and sub-GBZs exchanged after the transition.

can be understood as a combination of multiple twofold degeneracies. The change in topological invariants, such as the total vorticity, adheres to the additive principle over all twofold degeneracies. These arguments about the braiding phase transition generalize straightforwardly to topological transitions with arbitrary DPs and OBC band braidings.

An illustrated model. We study the following 1D non-Hermitian tight-binding model under OBC as an example of the continuity criterion, the OBC band braiding, and the topological transitions:

$$\hat{\mathcal{H}}_{br} = \sum_j [\mathbf{c}_j^\dagger \mathcal{M} \mathbf{c}_j + \mathbf{c}_j^\dagger \mathcal{T}_p \mathbf{c}_{j+1} + \mathbf{c}_{j+1}^\dagger \mathcal{T}_m \mathbf{c}_j], \tag{6}$$

where $\mathbf{c}_j$ is the annihilation operator at site j with $n = 2$ internal degrees of freedom, e.g., spins or sublattices, and we parametrize the hopping matrices as

$$\mathcal{M} = \begin{pmatrix} \lambda_3 & -im \\ im & -\lambda_3 \end{pmatrix},$$
$$\mathcal{T}_p = \begin{pmatrix} t_p + \lambda_1 & -t_a \\ t_a & t_p - \lambda_1 \end{pmatrix}, \quad \mathcal{T}_m = \begin{pmatrix} t_m + \lambda_2 & t_a \\ -t_a & t_m - \lambda_2 \end{pmatrix}. \tag{7}$$

The corresponding Laurent polynomial reads:

$$\mathcal{H}_{br}(\beta) = \begin{pmatrix} h_1(\beta) + h_2(\beta) & -h_0(\beta) \\ h_0(\beta) & h_1(\beta) - h_2(\beta) \end{pmatrix}, \tag{8}$$

where $h_0(\beta) = t_a(\beta - \beta^{-1}) + im$, $h_1(\beta) = t_p\beta + t_m\beta^{-1}$, and $h_2(\beta) = \lambda_1\beta + \lambda_2\beta^{-1} + \lambda_3$. Next, we explore its band braidings and topological transitions. For simplicity, we set $\lambda_1 = \lambda_2 = 0$, $t_p = 0.15$, $t_m = 0.85$, $t_a = 0.2$, $m = 0.1$, and vary λ_3 in the main text and leave more general cases to the Supplemental Material [93].

Applying our continuity criterion, we obtain the two OBC bands E_1 (blue) and E_2 (magenta) and their respective sub-GBZs as shown in Fig. 2. The bands' braiding topology is visible and distinguishable in the $(\mathrm{Re}(E), \mathrm{Im}(E), \theta)$ 3D space: the Hopf link of the separated bands [Fig. 2(a)] transforms into an unlink of the separated [Figs. 2(c)] or isolated [Figs. 2(d)] bands as λ_3 is gradually increased. The topological transition occurs with the emergence of two stable EPs where the two OBC bands meet [Fig. 2(b)]. Each EP contributes to a $\Delta\nu_e = -1/2$ change to the vorticity, which alters from $\nu_h = 1$ of the Hopf link to $\nu_u = 0$ of the unlink and sufficiently distinguishes the braiding topology.

Interestingly, as the red points on the two bands of the Hopf link approach [Fig. 2(a1)] and touch at the EPs [yellow points in Fig. 2(b1)], the bands switch partners—their parts between the EPs; see Fig. 2(c1). This band exchange is also apparent from the sub-GBZ view, where the sub-GBZs $\mathcal{C}_1$ and $\mathcal{C}_2$ touches at the topological transition and switch their portions between the two EPs [Figs. 2(a2) to 2(c2)]. We note that such an exchange requires a unified starting point for the sub-GBZs, say, an identical convention for β_1 and β_2's argument θ, so that the sub-GBZs remain continuous and well defined across the transition. For example, the green and orange points are $\theta = -\pi$ for the respective bands, regardless before or after the transition.

One interesting property under OBC is that each point (except a few endpoints) on its spectrum has to be visited (at least) twice [27,28]. Correspondingly, we mark the spectral flows along the OBC bands as $\theta \in [-\pi, \pi]$ traverses its range. Each point (exclusion of endpoints) on the Hopf link bands is visited twice. After the topological transition, however, the flow is intercepted and interchanged between the bands, each of which only visited the central loop once. It is their overlap that ensures the two-visit rule and unique for multiband OBC systems. Also, as the OBC bands touch at the EPs, the two-visit rule gives rise to two natural choices of flow directions and exchange partners; see the Supplemental Material for further discussions.

When λ_3 equals zero, on the other hand, Eq. (8) reduces to the model in Ref. [92]. The two sub-GBZs overlap, and as m is varied, the Hopf link and unlink are separated by a topological transition through a UDP, which splits into two EPs upon a small perturbation, e.g., a small λ_3.

Discussions and conclusions. We have proposed a continuity criterion to separate the respective sub-GBZs and non-Bloch bands of non-Hermitian multiband quantum systems under OBC. This allowed us to build their homotopic characterizations—braiding topology, such as the total vorticity over the OBC bands, and the intermediate topological transitions signaled by emergent DPs. We have also demonstrated our conclusions in an example non-Hermitian two-band model.

We have discovered that non-Hermitian open-boundary bands undergo part exchanges when the system transitions through specific EPs. Remarkably, this phenomenon also exists within the non-Hermitian Bloch bands, though it had remained unidentified until now. We have assumed closed sub-GBZs $\mathcal{C}_i$ homeomorphic to S^1 in the main text, yet our continuity criterion and braiding topology, homotopic characterization of B_n instead of PB_n, also remain valid for more subtle scenarios with intertwined sub-GBZs, as we discuss in the Supplemental Material [93]. Our analysis also does not depend on symmetries, whose participation in further topological classifications of the non-Bloch bands is an interesting open question for future studies.

Acknowledgments. We thank Kunkun Wang and Shu-Xuan Wang for the helpful discussions and comments. We acknowledge support from the National Key R&D Program of China (Grant No. 2022YFA1403700) and the National Natural Science Foundation of China (Grants No. 12174008 and No. 92270102).

[1] J. J. Quinn and K.-S. Yi, *Solid State Physics: Principles and Modern Applications* (Springer International Publishing, Cham, 2018).
[2] P. Phillips, *Advanced Solid State Physics*, 2nd ed. (Cambridge University Press, Cambridge, 2012).
[3] J. Negele, *Quantum Many-particle Systems* (CRC Press, Boca Raton, 1998).
[4] G. D. Mahan, *Many-Particle Physics* (Springer, New York, NY, 2000).
[5] A. Altland and B. D. Simons, *Condensed Matter Field Theory* (Cambridge University Press, Cambridge, 2010).
[6] E. Fradkin, *Field Theories of Condensed Matter Physics* (Cambridge University Press, Cambridge, 2013).
[7] N. Nagaosa and S. Heusler, *Quantum Field Theory in Condensed Matter Physics*, Theoretical and Mathematical Physics (Springer Berlin, Heidelberg, 2013).
[8] A. Yuto, G. Zongping, and U. Masahito, Non-Hermitian physics, Adv. Phys. **69**, 249 (2020).
[9] E. J. Bergholtz, J. C. Budich, and F. K. Kunst, Exceptional topology of non-Hermitian systems, Rev. Mod. Phys. **93**, 015005 (2021).
[10] R. Lin, T. Tai, L. Li, and C. H. Lee, Topological non-Hermitian skin effect, Front. Phys. **18**, 53605 (2023).
[11] N. Okuma and M. Sato, Non-Hermitian topological phenomena: A review, Annu. Rev. Condens. Matter Phys. **14**, 83 (2023).
[12] F. K. Kunst, E. Edvardsson, J. C. Budich, and E. J. Bergholtz, Biorthogonal bulk-boundary correspondence in non-Hermitian systems, Phys. Rev. Lett. **121**, 026808 (2018).
[13] Z. Gong, Y. Ashida, K. Kawabata, K. Takasan, S. Higashikawa, and M. Ueda, Topological phases of non-Hermitian systems, Phys. Rev. X **8**, 031079 (2018).
[14] K. Kawabata, K. Shiozaki, M. Ueda, and M. Sato, Symmetry and topology in non-Hermitian physics, Phys. Rev. X **9**, 041015 (2019).

[15] N. Okuma, K. Kawabata, K. Shiozaki, and M. Sato, Topological origin of non-Hermitian skin effects, Phys. Rev. Lett. **124**, 086801 (2020).
[16] D. S. Borgnia, A. J. Kruchkov, and R.-J. Slager, Non-Hermitian boundary modes and topology, Phys. Rev. Lett. **124**, 056802 (2020).
[17] T. Tai and C. H. Lee, Zoology of non-Hermitian spectra and their graph topology, Phys. Rev. B **107**, L220301 (2023).
[18] G. Yang, Y.-K. Li, Y. Fu, Z. Wang, and Y. Zhang, Complex semiclassical theory for non-Hermitian quantum systems, Phys. Rev. B **109**, 045110 (2024).
[19] V. M. Martinez Alvarez, J. E. Barrios Vargas, and L. E. F. Foa Torres, Non-Hermitian robust edge states in one dimension: Anomalous localization and eigenspace condensation at exceptional points, Phys. Rev. B **97**, 121401(R) (2018).
[20] S. Yao and Z. Wang, Edge states and topological invariants of non-Hermitian systems, Phys. Rev. Lett. **121**, 086803 (2018).
[21] K. Yokomizo and S. Murakami, Non-bloch band theory of non-Hermitian systems, Phys. Rev. Lett. **123**, 066404 (2019).
[22] C. H. Lee and R. Thomale, Anatomy of skin modes and topology in non-Hermitian systems, Phys. Rev. B **99**, 201103(R) (2019).
[23] K. Zhang, Z. Yang, and C. Fang, Correspondence between winding numbers and skin modes in non-Hermitian systems, Phys. Rev. Lett. **125**, 126402 (2020).
[24] Z. Yang, K. Zhang, C. Fang, and J. Hu, Non-Hermitian bulk-boundary correspondence and auxiliary generalized brillouin zone theory, Phys. Rev. Lett. **125**, 226402 (2020).
[25] Y. Fu and S. Wan, Degeneracy and defectiveness in non-Hermitian systems with open boundary, Phys. Rev. B **105**, 075420 (2022).
[26] Y. Fu and Y. Zhang, Anatomy of open-boundary bulk in multiband non-Hermitian systems, Phys. Rev. B **107**, 115412 (2023).
[27] D. Wu, J. Xie, Y. Zhou, and J. An, Connections between the open-boundary spectrum and the generalized brillouin zone in non-Hermitian systems, Phys. Rev. B **105**, 045422 (2022).
[28] Y.-M. Hu, H.-Y. Wang, Z. Wang, and F. Song, Geometric origin of non-bloch $\mathcal{PT}$ symmetry breaking, Phys. Rev. Lett. **132**, 050402 (2024).
[29] L. Xiao, T. Deng, K. Wang, G. Zhu, Z. Wang, W. Yi, and P. Xue, Non-Hermitian bulk–boundary correspondence in quantum dynamics, Nat. Phys. **16**, 761 (2020).
[30] A. Stegmaier, S. Imhof, T. Helbig, T. Hofmann, C. H. Lee, M. Kremer, A. Fritzsche, T. Feichtner, S. Klembt, S. Höfling, I. Boettcher, I. C. Fulga, L. Ma, O. G. Schmidt, M. Greiter, T. Kiessling, A. Szameit, and R. Thomale, Topological defect engineering and $\mathcal{PT}$ symmetry in non-Hermitian electrical circuits, Phys. Rev. Lett. **126**, 215302 (2021).
[31] L. Xiao, T. Deng, K. Wang, Z. Wang, W. Yi, and P. Xue, Observation of non-bloch parity-time symmetry and exceptional points, Phys. Rev. Lett. **126**, 230402 (2021).
[32] K. Wang, A. Dutt, K. Y. Yang, C. C. Wojcik, J. Vučković, and S. Fan, Generating arbitrary topological windings of a non-Hermitian band, Science **371**, 1240 (2021).
[33] W. Wang, X. Wang, and G. Ma, Non-Hermitian morphing of topological modes, Nature (London) **608**, 50 (2022).
[34] Q. Liang, D. Xie, Z. Dong, H. Li, H. Li, B. Gadway, W. Yi, and B. Yan, Dynamic signatures of non-Hermitian skin effect and topology in ultracold atoms, Phys. Rev. Lett. **129**, 070401 (2022).
[35] T. Helbig, T. Hofmann, S. Imhof, M. Abdelghany, T. Kiessling, L. W. Molenkamp, C. H. Lee, A. Szameit, M. Greiter, and R. Thomale, Generalized bulk–boundary correspondence in non-Hermitian topolectrical circuits, Nat. Phys. **16**, 747 (2020).
[36] X. Zhang, F. Zangeneh-Nejad, Z.-G. Chen, M.-H. Lu, and J. Christensen, A second wave of topological phenomena in photonics and acoustics, Nature (London) **618**, 687 (2023).
[37] L. Xiao, W.-T. Xue, F. Song, Y.-M. Hu, W. Yi, Z. Wang, and P. Xue, Observation of non-Hermitian edge burst in quantum dynamics, Phys. Rev. Lett. **133**, 070801 (2024).
[38] M. Z. Hasan and C. L. Kane, *Colloquium*: Topological insulators, Rev. Mod. Phys. **82**, 3045 (2010).
[39] X.-L. Qi and S.-C. Zhang, Topological insulators and superconductors, Rev. Mod. Phys. **83**, 1057 (2011).
[40] B. A. Bernevig and T. L. Hughes, *Topological Insulators and Topological Superconductors* (Princeton University Press, Princeton, 2013).
[41] C.-K. Chiu, J. C. Y. Teo, A. P. Schnyder, and S. Ryu, Classification of topological quantum matter with symmetries, Rev. Mod. Phys. **88**, 035005 (2016).
[42] T. Liu, Y.-R. Zhang, Q. Ai, Z. Gong, K. Kawabata, M. Ueda, and F. Nori, Second-order topological phases in non-Hermitian systems, Phys. Rev. Lett. **122**, 076801 (2019).
[43] K. Kawabata, M. Sato, and K. Shiozaki, Higher-order non-Hermitian skin effect, Phys. Rev. B **102**, 205118 (2020).
[44] R. Okugawa, R. Takahashi, and K. Yokomizo, Second-order topological non-Hermitian skin effects, Phys. Rev. B **102**, 241202(R) (2020).
[45] Y. Fu, J. Hu, and S. Wan, Non-Hermitian second-order skin and topological modes, Phys. Rev. B **103**, 045420 (2021).
[46] W. Zhu and J. Gong, Hybrid skin-topological modes without asymmetric couplings, Phys. Rev. B **106**, 035425 (2022).
[47] K. Zhang, Z. Yang, and C. Fang, Universal non-Hermitian skin effect in two and higher dimensions, Nat. Commun. **13**, 2496 (2022).
[48] Y. Li, C. Liang, C. Wang, C. Lu, and Y.-C. Liu, Gain-loss-induced hybrid skin-topological effect, Phys. Rev. Lett. **128**, 223903 (2022).
[49] L. S. Palacios, S. Tchoumakov, M. Guix, I. Pagonabarraga, S. Sánchez, and A. G. Grushin, Guided accumulation of active particles by topological design of a second-order skin effect, Nat. Commun. **12**, 4691 (2021).
[50] D. Zou, T. Chen, W. He, J. Bao, C. H. Lee, H. Sun, and X. Zhang, Observation of hybrid higher-order skin-topological effect in non-Hermitian topolectrical circuits, Nat. Commun. **12**, 7201 (2021).
[51] H.-Y. Wang, F. Song, and Z. Wang, Amoeba formulation of non-bloch band theory in arbitrary dimensions, Phys. Rev. X **14**, 021011 (2024).
[52] H. Hu, Topological origin of non-Hermitian skin effect in higher dimensions and uniform spectra, Sci. Bull. (2024).
[53] Y. Xiong and H. Hu, Graph morphology of non-Hermitian bands, Phys. Rev. B **109**, L100301 (2024).
[54] L. Li, C. H. Lee, and J. Gong, Impurity induced scale-free localization, Commun. Phys. **4**, 42 (2021).

[55] C.-X. Guo, X. Wang, H. Hu, and S. Chen, Accumulation of scale-free localized states induced by local non-Hermiticity, Phys. Rev. B **107**, 134121 (2023).

[56] B. Li, H.-R. Wang, F. Song, and Z. Wang, Scale-free localization and $\mathcal{PT}$ symmetry breaking from local non-Hermiticity, Phys. Rev. B **108**, L161409 (2023).

[57] P. Molignini, O. Arandes, and E. J. Bergholtz, Anomalous skin effects in disordered systems with a single non-Hermitian impurity, Phys. Rev. Res. **5**, 033058 (2023).

[58] Y. Fu and Y. Zhang, Hybrid scale-free skin effect in non-Hermitian systems: A transfer matrix approach, Phys. Rev. B **108**, 205423 (2023).

[59] X. Xie, G. Liang, F. Ma, Y. Du, Y. Peng, E. Li, H. Chen, L. Li, F. Gao, and H. Xue, Observation of scale-free localized states induced by non-Hermitian defects, Phys. Rev. B **109**, L140102 (2024).

[60] C. Kassel, O. Dodane, and V. Turaev, *Braid Groups*, Graduate Texts in Mathematics (Springer, New York, 2008).

[61] L. Kauffman, *Knots and Physics*, 4th ed., Series on Knots and Everything: Vol. 53 (World Scientific, Singapore, 2013).

[62] W. Chen, H.-Z. Lu, and J.-M. Hou, Topological semimetals with a double-helix nodal link, Phys. Rev. B **96**, 041102(R) (2017).

[63] Z. Yan, R. Bi, H. Shen, L. Lu, S.-C. Zhang, and Z. Wang, Nodal-link semimetals, Phys. Rev. B **96**, 041103(R) (2017).

[64] R. Bi, Z. Yan, L. Lu, and Z. Wang, Nodal-knot semimetals, Phys. Rev. B **96**, 201305(R) (2017).

[65] C. H. Lee, A. Sutrisno, T. Hofmann, T. Helbig, Y. Liu, Y. S. Ang, L. K. Ang, X. Zhang, M. Greiter, and R. Thomale, Imaging nodal knots in momentum space through topolectrical circuits, Nat. Commun. **11**, 4385 (2020).

[66] K. Ding, G. Ma, Z. Q. Zhang, and C. T. Chan, Experimental demonstration of an anisotropic exceptional point, Phys. Rev. Lett. **121**, 085702 (2018).

[67] Z. Yang and J. Hu, Non-Hermitian Hopf-link exceptional line semimetals, Phys. Rev. B **99**, 081102(R) (2019).

[68] J. Carlström, M. Stålhammar, J. C. Budich, and E. J. Bergholtz, Knotted non-Hermitian metals, Phys. Rev. B **99**, 161115 (2019).

[69] M. Stålhammar, L. Rødland, G. Arone, J. C. Budich, and E. J. Bergholtz, Hyperbolic nodal band structures and knot invariants, SciPost Phys. **7**, 019 (2019).

[70] Z. Yang, C.-K. Chiu, C. Fang, and J. Hu, Jones polynomial and knot transitions in Hermitian and non-Hermitian topological semimetals, Phys. Rev. Lett. **124**, 186402 (2020).

[71] E. Yang, B. Yang, O. You, H.-C. Chan, P. Mao, Q. Guo, S. Ma, L. Xia, D. Fan, Y. Xiang, and S. Zhang, Observation of non-Abelian nodal links in photonics, Phys. Rev. Lett. **125**, 033901 (2020).

[72] M. Stålhammar and E. J. Bergholtz, Classification of exceptional nodal topologies protected by $\mathcal{PT}$ symmetry, Phys. Rev. B **104**, L201104 (2021).

[73] X. Zhang, G. Li, Y. Liu, T. Tai, R. Thomale, and C. H. Lee, Tidal surface states as fingerprints of non-Hermitian nodal knot metals, Commun. Phys. **4**, 47 (2021).

[74] Y. S. S. Patil, J. Höller, P. A. Henry, C. Guria, Y. Zhang, L. Jiang, N. Kralj, N. Read, and J. G. E. Harris, Measuring the knot of non-Hermitian degeneracies and non-commuting braids, Nature (London) **607**, 271 (2022).

[75] K. Ding, C. Fang, and G. Ma, Non-Hermitian topology and exceptional-point geometries, Nat. Rev. Phys. **4**, 745 (2022).

[76] H. Hu, S. Sun, and S. Chen, Knot topology of exceptional point and non-Hermitian no-go theorem, Phys. Rev. Res. **4**, L022064 (2022).

[77] R.-Y. Zhang, X. Cui, W.-J. Chen, Z.-Q. Zhang, and C. T. Chan, Symmetry-protected topological exceptional chains in non-Hermitian crystals, Commun. Phys. **6**, 169 (2023).

[78] C.-X. Guo, S. Chen, K. Ding, and H. Hu, Exceptional non-Abelian topology in multiband non-Hermitian systems, Phys. Rev. Lett. **130**, 157201 (2023).

[79] J.-Z. Li, K. Bai, C. Guo, T.-R. Liu, L. Fang, D. Wan, and M. Xiao, Braiding topology of symmetry-protected degeneracy points in non-Hermitian systems, Phys. Rev. B **109**, L041102 (2024).

[80] C. C. Wojcik, X.-Q. Sun, T. c. v. Bzdušek, and S. Fan, Homotopy characterization of non-Hermitian hamiltonians, Phys. Rev. B **101**, 205417 (2020).

[81] Z. Li and R. S. K. Mong, Homotopical characterization of non-Hermitian band structures, Phys. Rev. B **103**, 155129 (2021).

[82] H. Hu and E. Zhao, Knots and non-Hermitian bloch bands, Phys. Rev. Lett. **126**, 010401 (2021).

[83] K. Wang, A. Dutt, C. C. Wojcik, and S. Fan, Topological complex-energy braiding of non-Hermitian bands, Nature (London) **598**, 59 (2021).

[84] C. C. Wojcik, K. Wang, A. Dutt, J. Zhong, and S. Fan, Eigenvalue topology of non-Hermitian band structures in two and three dimensions, Phys. Rev. B **106**, L161401 (2022).

[85] M.-M. Cao, K. Li, W.-D. Zhao, W.-X. Guo, B.-X. Qi, X.-Y. Chang, Z.-C. Zhou, Y. Xu, and L.-M. Duan, Probing complex-energy topology via non-Hermitian absorption spectroscopy in a trapped ion simulator, Phys. Rev. Lett. **130**, 163001 (2023).

[86] Z. Li, K. Ding, and G. Ma, Eigenvalue knots and their isotopic equivalence in three-state non-Hermitian systems, Phys. Rev. Res. **5**, 023038 (2023).

[87] W. B. Rui, Y. X. Zhao, and Z. D. Wang, Hermitian topologies originating from non-Hermitian braidings, Phys. Rev. B **108**, 165105 (2023).

[88] K. Yang, Z. Li, J. L. K. König, L. Rødland, M. Stralhammar, and E. J. Bergholtz, Homotopy, symmetry, and non-Hermitian band topology, Rep. Prog. Phys. **87**, 078002 (2024).

[89] Z. Pang, B. T. T. Wong, J. Hu, and Y. Yang, Synthetic non-Abelian gauge fields for non-Hermitian systems, Phys. Rev. Lett. **132**, 043804 (2024).

[90] J. Chen, Z. Wang, Y.-T. Tan, C. Wang, and J. Ren, Machine learning of knot topology in non-Hermitian band braids, Commun. Phys. **7**, 209 (2024).

[91] H. Wang, L. Fan, and S. Fan, One-dimensional non-Hermitian band structures as Riemann surfaces, arXiv:2401.11661 [math-ph].

[92] Y. Li, X. Ji, Y. Chen, X. Yan, and X. Yang, Topological energy braiding of non-Bloch bands, Phys. Rev. B **106**, 195425 (2022).

[93] See Supplemental Material at http://link.aps.org/supplemental/10.1103/PhysRevB.110.L121401 for detailed algorithm for the continuity criterion, more generic examples of open-boundary band braiding, and further discussions on vorticity, DP stability, and additional choices at transition under OBCs.

[94] For simplicity, we have set the lattice constant to 1.

[95] L. Li and C. H. Lee, Non-Hermitian pseudo-gaps, Sci. Bull. **67**, 685 (2022).
[96] The continuity condition is exact in the thermodynamic limit; in practice, however, we must set a numerical precision threshold for the ε_i variations in finite-size calculations.
[97] I. M. Gelfand, M. M. Kapranov, and A. V. Zelevinsky, Discriminants and resultants for polynomials in one variable, *Discriminants, Resultants, and Multidimensional Determinants* (Birkhäuser, Boston, MA, 1994), pp. 397–425.
[98] D. A. Cox, J. Little, and D. O'shea, Resultants, *Using Algebraic Geometry* (Springer, New York, NY, 2005), pp. 77–136.
[99] We have unified our references of links and knots as knots for simplicity.
[100] The vorticity expression is always well defined: the derivative of $\varepsilon_i - \varepsilon_j$ may be discontinuous at cusps or bifurcation points of the spectrum, yet such singularity originates from the absolute value instead of the argument.
[101] E. Witten, Quantum field theory and the Jones polynomial, Commun. Math. Phys. **121**, 351 (1989).
[102] J. Fröhlich and C. King, The Chern-Simons theory and knot polynomials, Commun. Math. Phys. **126**, 167 (1989).
[103] P. Ozsváth and Z. Szabó, Holomorphic disks and knot invariants, Adv. Math. **186**, 58 (2004).
[104] H. Shen, B. Zhen, and L. Fu, Topological band theory for non-Hermitian hamiltonians, Phys. Rev. Lett. **120**, 146402 (2018).
[105] W. D. Heiss, The physics of exceptional points, J. Phys. A: Math. Theor. **45**, 444016 (2012).
[106] T. E. Lee, Anomalous edge state in a non-Hermitian lattice, Phys. Rev. Lett. **116**, 133903 (2016).
[107] Z. Yang, A. P. Schnyder, J. Hu, and C.-K. Chiu, Fermion doubling theorems in two-dimensional non-Hermitian systems for Fermi points and exceptional points, Phys. Rev. Lett. **126**, 086401 (2021).